JACS
JOURNAL OF THE AMERICAN CHEMICAL SOCIETY

ARTICLE

pubs.acs.org/JACS

High-Valent Uranium Alkyls: Evidence for the Formation of $U^{VI}(CH_2SiMe_3)_6$

Skye Fortier,[†] Justin R. Walensky,[‡] Guang Wu,[†] and Trevor W. Hayton*[,†]

[†]Department of Chemistry and Biochemistry, University of California, Santa Barbara, California 93106, United States

[‡]Department of Chemistry, University of Missouri, Columbia, Missouri 65211, United States

Supporting Information

ABSTRACT: Oxidation of $[Li(DME)_3][U(CH_2SiMe_3)_5]$ with 0.5 equiv of I_2, followed by immediate addition of $LiCH_2SiMe_3$, affords the high-valent homoleptic U(V) alkyl complex $[Li(THF)_4][U(CH_2SiMe_3)_6]$ (**1**) in 82% yield. In the solid-state, **1** adopts an octahedral geometry as shown by X-ray crystallographic analysis. Addition of 2 equiv of *tert*-butanol to $[Li(DME)_3][U(CH_2SiMe_3)_5]$ generates the heteroleptic U(IV) complex $[Li(DME)_3][U(O^tBu)_2(CH_2SiMe_3)_3]$ (**2**) in high yield. Treatment of **2** with AgOTf fails to produce a U(V) derivative, but instead affords the U(IV) complex $(Me_3SiCH_2)Ag(\mu\text{-}CH_2SiMe_3)U(CH_2SiMe_3)(O^tBu)_2(DME)$ (**3**) in 64% yield. Complex **3** has been characterized by X-ray crystallography and is marked by a uranium−silver bond. In contrast, oxidation of **2** can be achieved via reaction with 0.5 equiv of Me_3NO, producing the heteroleptic U(V) complex $[Li(DME)_3][U(O^tBu)_2(CH_2SiMe_3)_4]$ (**4**) in moderate yield. We have also attempted the one-electron oxidation of complex **1**. Thus, oxidation of **1** with $U(O^tBu)_6$ results in formation of a rare U(VI) alkyl complex, $U(CH_2SiMe_3)_6$ (**6**), which is only stable below −25 °C. Additionally, the electronic properties of **1**−**4** have been assessed by SQUID magnetometry, while a DFT analysis of complexes **1** and **6** is also provided.

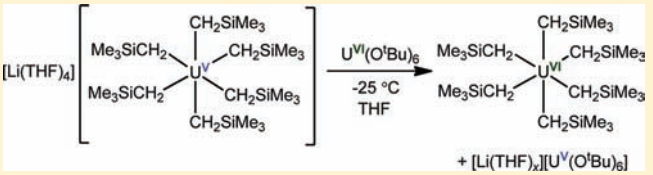

INTRODUCTION

High-valent, homoleptic organometallic complexes of the type $[MR_6]^n$ (R = alkyl, H; n = 0, −1) have been the focus of intense theoretical and experimental scrutiny.[1−16] These complexes are solely supported by σ-bonding interactions, which provides a unique opportunity to assay the electronic properties of the metal−ligand bond devoid of complicating π-contributions. Simple electrostatic models, such as VSEPR, dictate that these complexes should adopt an O_h molecular geometry to minimize intramolecular ligand−ligand repulsions.[15] However, more rigorous molecular orbital and valence bond analyses predict an energetic preference for lower geometries, namely trigonal prismatic with D_{3h} or C_{3v} symmetry.[1−3,5,12−14] According to molecular orbital theory, the distortion away from O_h allows for greater metal d-orbital involvement in the metal−ligand bonding,[1−3,5,7,8,10,17] resulting in a greater covalent character in the M−C bond and a strengthening of the σ-interaction.[2,3] This distortion is only expected for high oxidation state d^0 and d^1 systems, as the presence of more d-electrons forces the p-orbitals to participate in M−R bonding, which subsequently favors an octahedral geometry.[2,3,8,10]

Structural evidence supporting the molecular orbital analysis of $[MR_6]^n$-type complexes was first observed for $[Li(tmeda)]_2[ZrMe_6]$, which exhibits a trigonal prismatic D_{3h} geometry in the solid state.[11] Subsequently, the X-ray crystallographic determination of WMe_6 by Seppelt and Pfennig revealed a distorted trigonal prismatic C_{3v} geometry.[8,18,19] The homoleptic σ-bonded complexes $ReMe_6$ and $[Ta(C{\equiv}CSi^tBu_3)_6]^-$ also exhibit trigonal prismatic structures.[8,20]

In contrast to the d-block, the capacity of the actinide elements to engage in similar covalent metal−ligand interactions is unclear and remains an area of much discussion.[21−32] In this regard, the synthesis of an actinide analogue to WMe_6 could answer some of the fundamental questions concerning the participation of the 6d and 5f-orbitals in bonding.[33,34] However, U(VI) complexes featuring U−C σ-bonds are nearly nonexistent,[35] while U(V) complexes with U−C σ-bonds are also rare. Only a few examples are known, such as the U(V) octa(alkyl) uranates $[Li(dioxane)]_3[UR_8]$ (R = Me, $CH_2{}^tBu$, CH_2SiMe_3) reported by Wilkinson.[36,37] Unfortunately, characterization data for these complexes is limited and their formulation has since been questioned.[38] Other examples of U(V) complexes possessing uranium−carbon σ-interactions include $U[CH_2SiMe_2NSiMe_3]_2[N(SiMe_3)_2]$ and $[N(SiMe_3)]_2U(\mu\text{-}N)(\mu\text{-}CH_2SiMe_2NSiMe_3)U[N(SiMe_3)]_2$,[39,40] the imido supported metallocenes $(\eta^5\text{-}C_5Me_5)_2UR(=NAr)$ (R = Me, C_6H_5, C≡CPh; Ar = 2,6-$^iPr_2C_6H_3$),[41,42] and the cyano complex $[^nBu_4N]_2[(\eta^5\text{-}C_5Me_5)_2U(CN)_5]$.[43] High-valent uranium hydrides, such as UH_6, are also unknown. In fact, UH_6 is anticipated to readily undergo reductive elimination to afford UH_4 and H_2.[34] Interestingly, a molecular orbital analysis of UH_6 predicts it will adopt an O_h geometry when the 5f-orbitals are allowed to participate in metal−ligand bonding.[33,34] It must be noted, however, that this octahedral preference is rather weak, and several nonoctahedral geometries were calculated to be within 20 kJ·mol^{-1} of the O_h structure.[33]

Received: May 5, 2011
Published: June 22, 2011

Scheme 1

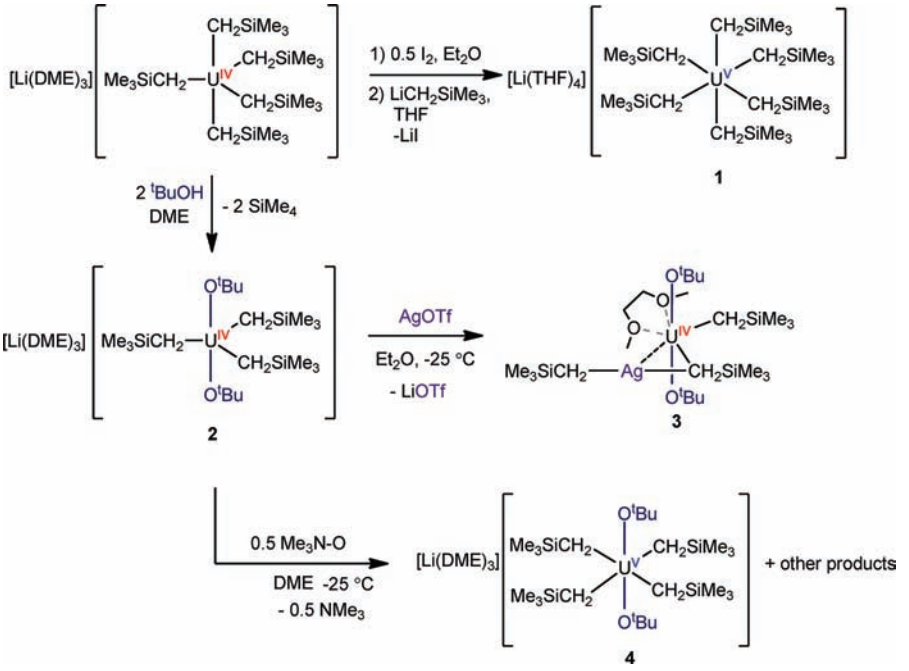

In this contribution, we describe our efforts to synthesize uranium complexes in the 5+ and 6+ oxidation states that are predominantly supported by U−C_{alkyl} bonds, and describe our endeavors to understand the electronic structure of these interactions utilizing density functional theory.

RESULTS AND DISCUSSION

Syntheses. We recently reported the syntheses of several homoleptic U(IV) alkyl complexes with the formulation $[UR_6]^{2-}$ (R = Me, $CH_2C_6H_5$) and $[UR_5]^-$ (R = $CH_2{}^tBu$, CH_2SiMe_3).[44] These materials appear well poised for further elaboration, and we are now exploring their utility as precursors to $[AnR_6]^n$-type complexes (R = alkyl, H; n = 0, −1). Addition of 0.5 equiv of I_2 to $[Li(DME)_3][U(CH_2SiMe_3)_5]$ in Et_2O at −25 °C, followed by immediate addition of 1 equiv of $LiCH_2SiMe_3$, results in formation of the deep-green homoleptic U(V) alkyl complex $[Li(THF)_4][U(CH_2SiMe_3)_6]$ (**1**), which can be isolated in 82% yield (Scheme 1). We postulate that the added equivalent of alkyl ligand serves to saturate the metal center and enhance the kinetic stability of the resulting U(V) complex. This methodology is similar to that employed in the synthesis of the homoleptic U(V) amido complex $[Li(DME)_3][U(NC_5H_{10})_6]$.[45] We also attempted the oxidation of the related hexamethyl complex $[Li(TMEDA)]_2[UMe_6]$.[44] However, treatment of cold solutions of $[Li(TMEDA)]_2[UMe_6]$ with 0.5 equiv of I_2, or 1 equiv of AgOTf, solely yielded intractable mixtures.

Single crystals of **1** suitable for X-ray analysis were grown from a hexane/Et_2O solution at −25 °C. Complex **1** crystallizes in the monoclinic space group $P2_1/c$, and its asymmetric unit contains two crystallographically independent uranium centers. The solid-state molecular structure of one full molecule is shown in Figure 1. In the solid-state, **1** crystallizes as a discrete cation/anion pair. The anionic U(V) center is coordinated by six methyltrimethylsilyl ligands in an octahedral geometry

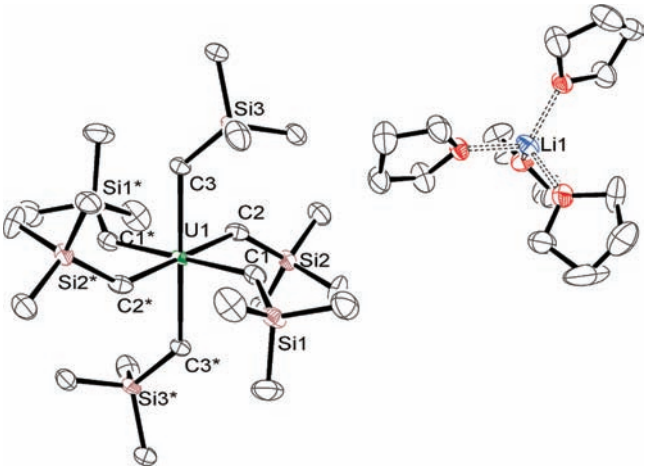

Figure 1. ORTEP diagram of $[Li(THF)_4][U(CH_2SiMe_3)_6]$ (**1**) with 50% probability ellipsoids. Asterisks indicate symmetry related atoms. Selected bond lengths (Å) and angles (deg): U1−C1 = 2.429(8), U1−C2 = 2.413(7), U1−C3 = 2.451(6), U1−C1−Si1 = 138.9(4), U1−C2−Si2 = 137.1(4), U1−C3−Si3 = 131.8(4), C1−U1−C2 = 89.5(3), C1−U1−C3 = 90.6(2), C2−U1−C3 = 86.0(2), C1−U1−C1* = 180.

(e.g., C1−U1−C2 = 89.5(3)°, C1−U1−C3 = 90.6(2)°, C2−U1−C3 = 86.0(2)°). Its U−C bond distances are U1−C1 = 2.429(8) Å, U1−C2 = 2.413(7) Å, and U1−C3 = 2.451(6) Å, while the corresponding U−C−Si bond angles are U1−C1−Si1 = 138.9(4)°, U1−C2−Si2 = 137.1(4)°, and U1−C3−Si3 = 131.8(4)°. Interestingly, the U−C bond lengths of **1** are nearly equivalent to the U−C distances (av. 2.46(1) Å) of its parent complex $[U(CH_2SiMe_3)_5]^-$,[44] despite the smaller radius of the U^{5+} ion. This may be due to the higher coordination number of **1** versus that of $[U(CH_2SiMe_3)_5]^-$, which is also

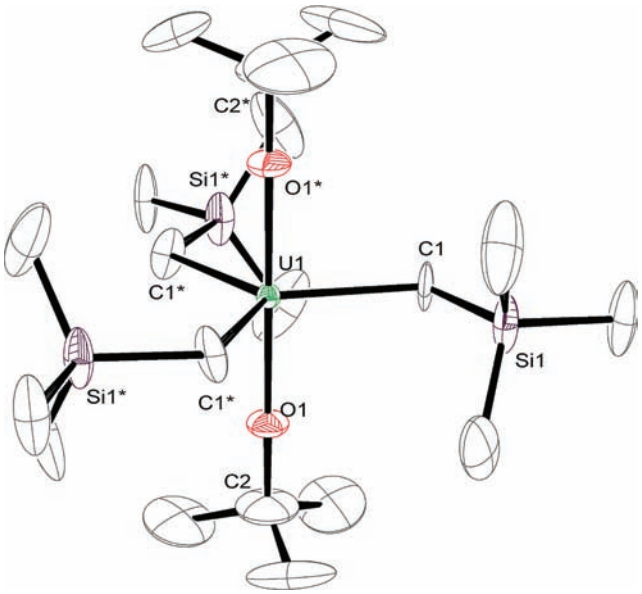

Figure 2. ORTEP diagram of $[Li(DME)_3][U(O^tBu)_2(CH_2SiMe_3)_3]$ (**2**) with 50% probability ellipsoids. $[Li(DME)_3]^+$ cation not shown. Asterisks indicate symmetry related atoms. Selected bond lengths (Å) and angles (deg): U1−C1 = 2.49(1), U1−O1 = 2.085(7), U1−C1−Si1 = 114.5(6), U1−O1−C2 = 180, C1−U1−O1 = 90.0(5), C1−U1−C1* = 120.

reflected in the larger U−C−Si bond angles of **1**, compared to those exhibited in $[U(CH_2SiMe_3)_5]^-$. To our knowledge, only two other pentavalent complexes possessing a $U-C_{alkyl}$ bond have been crystallographically characterized, namely the metallacycles $U[CH_2SiMe_2NSiMe_3]_2[N(SiMe_3)_2]$ and $[N(SiMe_3)]_2U(\mu\text{-}N)(\mu\text{-}CH_2SiMe_2NSiMe_3)U[N(SiMe_3)]_2$.[39,40] The latter features a U−C bond length (U−C = 2.427(8) Å) which is similar to those observed in **1**. Additionally, the structural characterization of **1** as an octahedral complex calls into question the octa-coordinate alkyl complexes reported by Wilkinson.[37] In our hands, addition of $LiCH_2SiMe_3$ to THF solutions of **1** does not generate higher-coordinate derivatives, such as $Li_3[U(CH_2SiMe_3)_8]$, but instead leaves **1** unchanged.

Complex **1** is highly soluble in ethereal solvents such as Et_2O and THF but completely insoluble in aliphatic solvents such as hexane. Its ^1H NMR spectrum in THF-d_8 displays two singlets at −8.19 and 0.86 ppm, in a 2:9 ratio, respectively, which are attributable to the methylene and methyl protons of the methyltrimethylsilyl ligand. The $^{13}C\{^1H\}$ NMR spectrum in THF-d_8 displays a single resonance at 42.2 ppm, corresponding to the methyl carbons of the methyltrimethylsilyl ligand, while the resonance for the methylene carbon was not observed. Its $^7Li\{^1H\}$ NMR spectrum exhibits a single resonance at 3.22 ppm. The UV−vis/NIR spectrum exhibits a dominant absorption band at 1462 nm, characteristic of other U(V) complexes,[41] further supporting the $5f^1$ electronic configuration.

Complex **1** can be stored indefinitely at −25 °C as a crystalline solid, but upon standing at room temperature, it slowly decomposes to a brown oil within two days. The thermal stability of **1** is much less than that of its parent complex, $[Li(DME)_3][U(CH_2SiMe_3)_5]$, which is stable in the solid state for several days at room temperature.[44] Furthermore, room temperature solutions of **1** in THF or DME decompose within several hours, providing $SiMe_4$ and trace amounts of $[Li(THF)_x][U(CH_2SiMe_3)_5]$, as the only detectable products by ^1H NMR spectroscopy. The observation of $[Li(THF)_x][U(CH_2SiMe_3)_5]$ in the reaction mixture suggests that its decomposition arises, in part, from M−C bond homolysis, a known decomposition pathway for high-valent alkyl complexes.[46,47] Complex **1** also rapidly decomposes in aromatic solvents, such as benzene or toluene, generating complex reaction mixtures.

We have also explored the synthesis of a heteroleptic high-valent organouranium complex, as a means of engendering greater thermal stability to these reactive materials. Addition of 2 equiv of ^{t}BuOH to $[Li(DME)_3][U(CH_2SiMe_3)_5]$ in DME affords $[Li(DME)_3][U(O^tBu)_2(CH_2SiMe_3)_3]$ (**2**) in 86% yield (Scheme 1). Storage of a dilute DME solution of **2** at −25 °C for several hours results in the deposition of pink crystals suitable for X-ray analysis. Complex **2** crystallizes as a discrete cation/anion pair in the trigonal space group $P\bar{3}1c$ (Figure 2). The anionic U(IV) center exhibits a trigonal bipyramidal geometry, in which three methyltrimethylsilyl ligands occupy the equatorial plane and two *tert*-butoxide groups occupy the axial positions. Additionally, the uranium center of **2** lies on a special position and the methyltrimethylsilyl ligands are disordered over two positions resulting in a three-fold rotation axis through the U1−O1−C2 vector. The U−C bond length (U1−C1 = 2.49(1) Å) is comparable to those observed in $[U(CH_2SiMe_3)_5]^-$,[44] while its U−C−Si bond angle (U1−C1−Si = 114.5(6)°) is slightly smaller. Furthermore, the U−O distance (U1−O1 = 2.085(7) Å) and U−O−C angle (U1−O1−C1 = 180°) in **2** are similar to the terminal uranium-alkoxide interactions in $[Li(THF)]_2[U(O^tBu)_6]$ (e.g., U−O = 2.137(9) Å; U−O−*C* = 171.3(9)°).[48]

Complex **2** is insoluble in arenes and nonpolar solvents, but partly soluble in ethereal solvents such as Et_2O and DME. Its ^1H NMR spectrum in THF-d_8 displays three resonances at −229.29, −33.28, and 90.37 ppm in a 6:27:18 ratio, respectively. The resonances at −229.29 and −33.28 ppm are assignable to the methylene and methyl protons, respectively, of the methyltrimethylsilyl groups, while the resonance at 90.37 ppm is assignable to the *tert*-butoxide ligand. Additionally, a singlet at 1.20 ppm is observed in the $^7Li\{^1H\}$ NMR spectrum.

As anticipated, complex **2** exhibits greater thermal stability than that observed for $[Li(DME)_3][U(CH_2SiMe_3)_5]$. For instance, **2** is stable in solution at room temperature for several days, whereas $[Li(DME)_3][U(CH_2SiMe_3)_5]$ decomposes over 24 h.[44] As a crystalline solid, **2** can be stored indefinitely at room temperature. However, in contrast to the reactivity observed for $[Li(DME)_3][U(CH_2SiMe_3)_5]$, addition of 0.5 equiv of I_2 to Et_2O solutions of **2** at −25 °C, followed by addition of 1 equiv of $LiCH_2SiMe_3$, does not generate a U(V) complex, but instead returns **2** as the only identifiable product. The failure to generate a U(V) species by this route prompted us to pursue other oxidants. Thus, treatment of an Et_2O suspension of **2** with AgOTf results in an immediate color change and formation of a pale-yellow solution concomitant with the deposition of a white powder. Removal of the solvent, followed by extraction into pentane and storage at −25 °C affords pink crystalline blocks of $(Me_3SiCH_2)Ag(\mu\text{-}CH_2SiMe_3)U(CH_2SiMe_3)(O^tBu)_2(DME)$ (**3**) in 64% yield (Scheme 1).

Complex **3** crystallizes in the monoclinic space group $P2_1/n$, and its solid-state molecular structure is shown in Figure 3. In the solid state, the uranium center in **3** exhibits a distorted pentagonal bipyramidal geometry, in which two *tert*-butoxide groups occupy the axial positions, while the equatorial plane is occupied by a molecule of DME, a terminal methyltrimethylsilyl group, a bridging methyltrimethylsilyl group, and a silver atom.

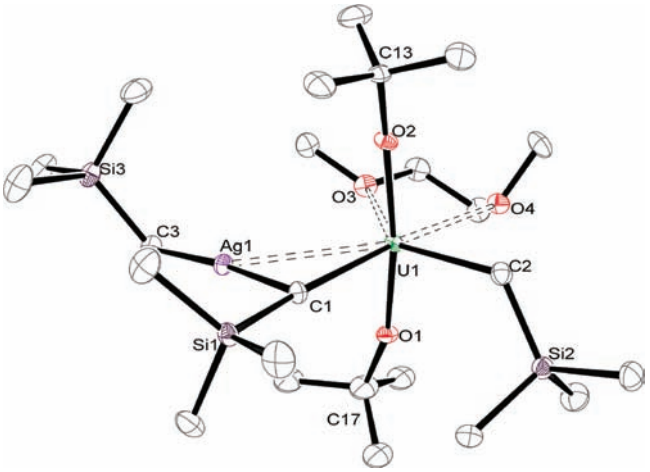

Figure 3. ORTEP diagram of $(Me_3SiCH_2)Ag(\mu\text{-}CH_2SiMe_3)$-$U(CH_2SiMe_3)(O^tBu)_2(DME)$ (**3**) with 50% probability ellipsoids. Selected bond lengths (Å) and angles (deg): Ag1−U1 = 3.1533(6), U1−C1 = 2.658(6), U1−C2 = 2.461(6), U1−O1 = 2.077(4), U1−O2 = 2.059(4), U1−O3 = 2.592(4), U1−O4 = 2.592(4), Ag1−C1 = 2.173(6), Ag1−C3 = 2.105(6), U1−C1−Si1 = 176.8(3), U1−C1−Ag1 = 80.8(2), U1−C2−Si2 = 124.7(3), U1−O1−C17 = 164.3(4), U1−O2−C13 = 167.4(4), C1−U1−C2 = 89.4(2), O1−U1−C2 = 100.0(2), C2−U1−O4 = 79.3(2), C1−Ag1−C3 = 174.3(3), Ag1−C1−Si1 = 118.2(3).

The terminal $U-C_{alkyl}$ (U1−C2 = 2.461(6) Å) and $U-O_{alkoxide}$ (U1−O1 = 2.077(4) Å, U1−O2 = 2.059(4) Å) bond distances are similar to those found for **2**. The silver center is linearly ligated (C1−Ag1−C3 = 174.3(3)°), a common geometry for Ag^+,[49−51] and exhibits Ag−C distances (Ag1−C1 = 2.173(6) Å, Ag1−C3 = 2.105(6)Å) similar to those of other known silver alkyls.[51] Owing to the bridging interaction in **3**, the U1−C1 bond (2.658(6) Å) is elongated with a near linear U1−C1−Si1 bond angle (176.8(3)°).

Interestingly, the bridging methyltrimethylsilyl ligand exhibits an acute U−C−Ag angle (U1−C1−Ag1 = 80.8(2)°), supporting the presence of an Ag−U contact. The Ag1−U1 = 3.1533(6) Å distance in **3** is considerably shorter than the sum of the covalent radii (3.41 Å),[52] further suggesting a metal−metal bond. Silver-metal bonds[50,53,54] are well documented for mid- to late-transition metals[49,55−58] but are unprecedented for uranium. In fact, actinide-metal bonds of any type are quite rare and limited to a handful of structurally characterized examples.[59−64] These argentophilic interactions are poorly understood,[53,55] but as silver is generally believed to act as an inner-sphere oxidant,[49,65,66] this interaction in **2** may represent an intermediate step in its oxidation by Ag^+. Consistent with this idea, solutions of **3** slowly decompose on standing at room temperature, resulting in the deposition of silver mirror and formation of $SiMe_4$ as the only detectable product by ^1H NMR spectroscopy. However, at −25 °C, **3** can be stored indefinitely as a solid or in solution.

The ^1H NMR spectrum of **3** in C_7D_8 exhibits two resonances at −24.13 and −18.95 ppm, in a 2:9 ratio, respectively, attributable to methylene and methyl protons of the uranium-coordinated terminal methyltrimethylsilyl group. An additional singlet, integrating to 18H, is observed at −15.71 ppm which we have assigned to the methyl protons of the $[Ag(CH_2SiMe_3)_2]^-$ moiety. The observation of a single resonance for the $[Ag(CH_2SiMe_3)_2]^-$ fragment suggests rapid exchange of its bridging and terminal alkyl ligands. A resonance corresponding to the methylene protons of the $[Ag(CH_2SiMe_3)_2]^-$ unit was not observed. Additionally, the ^1H NMR spectrum of **3** displays a singlet at 86.62 ppm attributable to the *tert*-butoxide ligands.

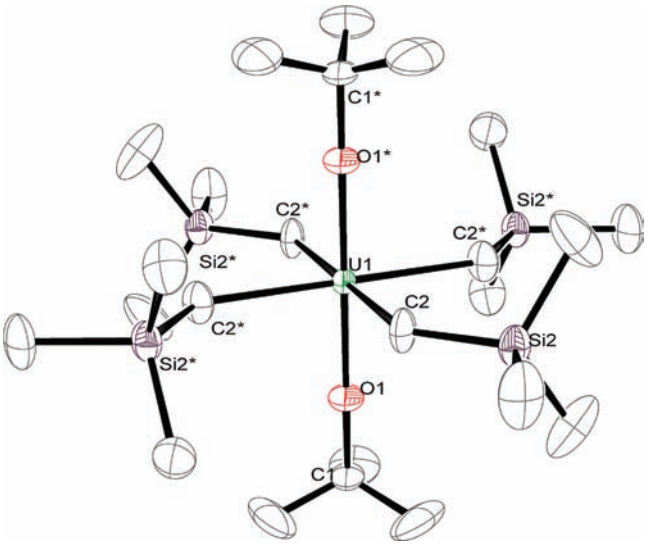

Figure 4. ORTEP diagram of $[Li(DME)_3][U(O^tBu)_2(CH_2SiMe_3)_4]$ (**4**·Et_2O) with 50% probability ellipsoids. $[Li(DME)_3]^+$ cation and Et_2O not shown. Asterisks indicate symmetry related atoms. Selected bond lengths (Å) and angles (deg): U1−C2 = 2.42(2), U1−O1 = 2.053(8), U1−C2−Si2 = 134. 9(8), U1−O1−C1 = 180, C2−U1−O1 = 90, C2−U1−C2* = 90.3(5).

We have pursued the reaction of **2** with other oxidants as a means of accessing a tractable pentavalent complex. Gratifyingly, addition of 0.5 equiv of trimethylamine-*N*-oxide (Me_3NO) to a suspension of **2** in DME rapidly generates a dark-red solution from which the heteroleptic U(V) complex $[Li(DME)_3][U(O^tBu)_2(CH_2SiMe_3)_4]$ (**4**) can be isolated in 43% yield (Scheme 1). Complex **4** is insoluble in arenes and nonpolar solvents but highly soluble in ethereal solvents, such Et_2O and DME. Its ^1H NMR spectrum in THF-d_8 displays three resonances at −0.79, −0.38, and 7.37 ppm occurring in a 36:8:18 ratio, respectively. The resonances at −0.79 and −0.38 ppm are assignable to the methyl and methylene protons of the methyltrimethylsilyl ligands, while the singlet at 7.37 ppm corresponds to the methyl protons of the *tert*-butoxide ligand. Consistent with its formulation, the $^7Li\{^1H\}$ NMR spectrum displays a single peak at 3.09 ppm. Complex **4** also possesses an increased thermal stability versus that exhibited by **1**, suggesting that the *tert*-butoxide ligands do impart a stabilizing effect. For instance, complex **4** is stable in solutions of THF-d_8 for several hours at room temperature, whereas complex **1** decomposes completely over that time period. After 48 h, however, **4** decomposes completely, providing $SiMe_4$ and trace amounts of **2** as the only identifiable products of decomposition.

Complex **4** crystallizes as the Et_2O solvate, **4**·Et_2O, in the tetragonal space group $P4_2/mmc$, and its solid-state molecular structure is shown in Figure 4. Complex **4**·Et_2O possesses an octahedral anionic U(V) center ligated by trans oriented *tert*-butoxide groups with four equatorially bound methyltrimethylsilyl ligands. Notably, the U−C (U1−C2 = 2.42(2) Å) and U−O (U1−O1 = 2.053(8) Å) bond distances in **4** are comparable to the corresponding bond lengths in **2**, which may be due to its higher coordination number. The U−C bond length in **4** is also comparable to the U−C distances in **1**.

Clearly, the oxidation of **2** by Me_3NO is a complicated process involving alkyl ligand scrambling and oxygen atom transfer.

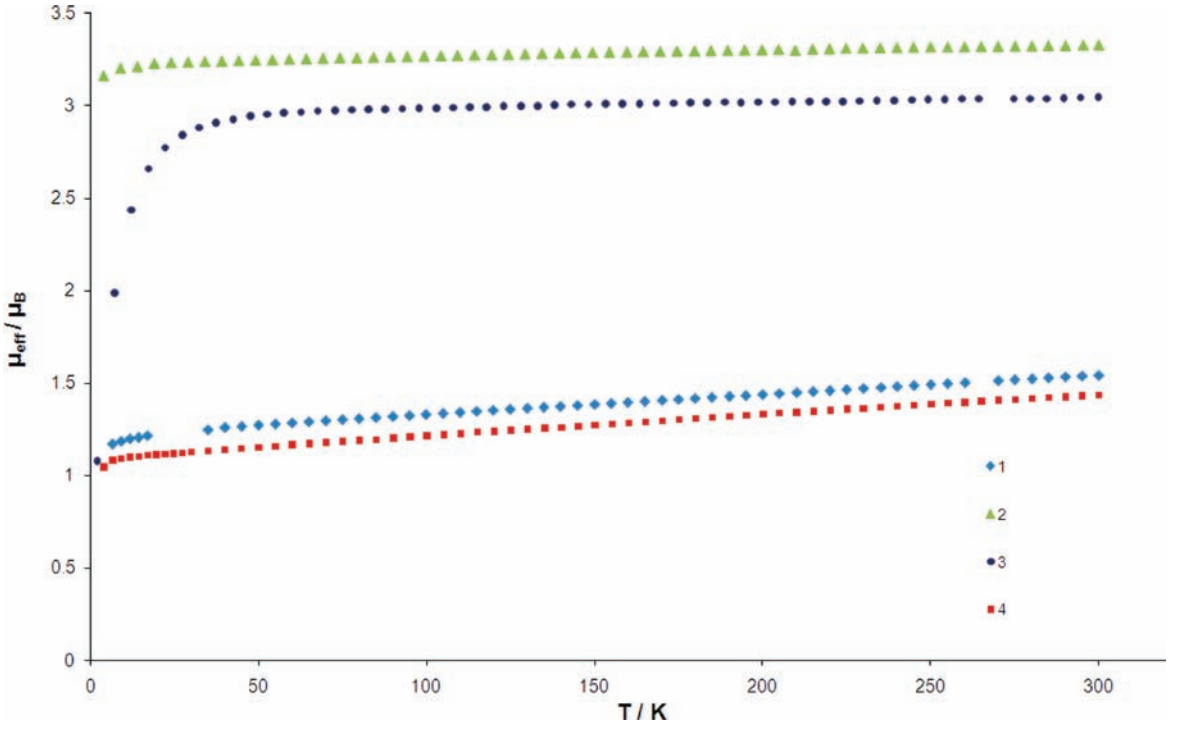

Figure 5. Temperature-dependent SQUID magnetization data for **1**−**4**.

We have endeavored to determine the fate of the oxygen atoms of the trimethylamine-*N*-oxide during the oxidation of **2** (Scheme 1) but have been unsuccessful thus far. However, it is likely that low isolated yield of **4** (43%) is partly a reflection of the presence of a sacrificial oxygen acceptor in the reaction mixture.

Magnetism. To confirm the U(V) oxidation state assignments for complexes **1** and **4**, their magnetic susceptibilities were investigated by SQUID magnetometry. A plot of their effective magnetic moments (μ_{eff}) versus temperature is shown in Figure 5. At 300 K, **1** and **4** possess μ_{eff} values of 1.54 μ_B and 1.44 μ_B, respectively, which are considerably smaller than the 2.54 μ_B calculated for the U^{5+} ion in a $^2F_{5/2}$ ground state.[67] These values are also lower than those generally observed for other U(V) complexes, which range from 1.9 to 2.5 μ_B at room temperature.[67−72] However, they are comparable to the 1.3 μ_B found for the homoleptic amido complex $[Li(DME)_3][U(NC_5H_{10})_6]$.[45] Decreased μ_{eff} values for uranium complexes are often attributed to ligand field quenching of the angular orbital momentum,[67,70,73−78] an effect which may be intensified by the strong field alkyl ligands of **1** and **4**. At lower temperatures, the μ_{eff} values of **1** and **4** decrease only slightly to 1.19 μ_B and 1.05 μ_B, respectively, at 4 K. This temperature response is in accord with the magnetic behavior normally observed for U(V).[67,69−72]

In comparison, complexes **2** and **3** exhibit larger μ_{eff} values, consistent with their lower U(IV) oxidation states. The μ_{eff} values for **2** and **3** are 3.33 μ_B and 3.05 μ_B, respectively, at room temperature. These values are only slightly smaller than the theoretical 3.54 μ_B anticipated for a free U(IV) ion in a $^3H_4$ ground state,[69,74,79] and similar to the 3.18 μ_B exhibited by $[Li(DME)_3][U(NC_5H_{10})_5]$ at 295 K.[45] Upon cooling, the μ_{eff} of **2** decreases slightly to 3.16 μ_B at 4 K. Notably, this behavior contrasts the strong temperature dependent response of most other U(IV) complexes, which typically trend toward singlet ground states at lower temperatures,[44,70,74,77,80−85] but this behavior is in line with that observed for other five coordinate U(IV) complexes, such as $[Li][UR_5]$ (R = CH_2SiMe_3, $CH_2{}^tBu$, NC_5H_{10}).[44,45] In contrast, the μ_{eff} value for **3** decreases to 2.91 μ_B at 38 K before dropping to 1.08 μ_B at 2 K, behavior that is more typical of U(IV), possibly reflecting the different coordination environments of **2** and **3**.

Electrochemistry. The solution phase redox properties of **1** and **4** were investigated by cyclic voltammetry. In THF at room temperature, the cyclic voltammogram of **1** displays a quasi-reversible redox feature at −1.22 V (vs $[Cp_2Fe]^{0/+}$) (Figure 6). We have assigned this feature to a U(VI)/U(V) redox couple. This potential is in accord with the U(VI)/U(V) redox values observed for other homoleptic, hexa-coordinate uranium complexes possessing strongly electron-donating ligands, such as $[U(O^tBu)_6]^{0/-}$ ($E_{1/2}$ = −1.12 V vs $[Cp_2Fe]^{0/+}$) and $[U(NC_5H_{10})_6]^{0/-}$ ($E_{1/2}$ = −1.51 V vs $[Cp_2Fe]^{0/+}$).[45,48,86] Scanning to negative potentials produces an irreversible reduction feature at approximately −3.0 V that we attribute to reduction to U(IV). The irreversibility of this feature is consistent with the structural changes anticipated to occur upon conversion of hexa-coordinate **1** to penta-coordinate $[U(CH_2SiMe_3)_5]^-$. In contrast to the electrochemistry observed for **1**, the cyclic voltammogram of **4** in THF at room temperature exhibits an oxidation feature at −1.17 V (vs $[Cp_2Fe]^{0/+}$) that is irreversible at low scan rates ($i_{p,a}/i_{p,c}$ = 1.9 at 100 mV/s). We have tentatively assigned this feature as a U(V)/U(VI) oxidation (see Supporting Information [SI]). At higher scan rates, the reversibility of the feature improves slightly ($i_{p,a}/i_{p,c}$ = 1.2 at 500 mV/s). Overall however, our electrochemistry results suggest that the product generated by oxidation of **4** is significantly less stable than that generated upon oxidation of **1**.

Given the results of our electrochemical study, we have pursued the oxidation of both **1** and **4** by chemical methods. In particular, we first targeted the use of "innocent" outer-sphere

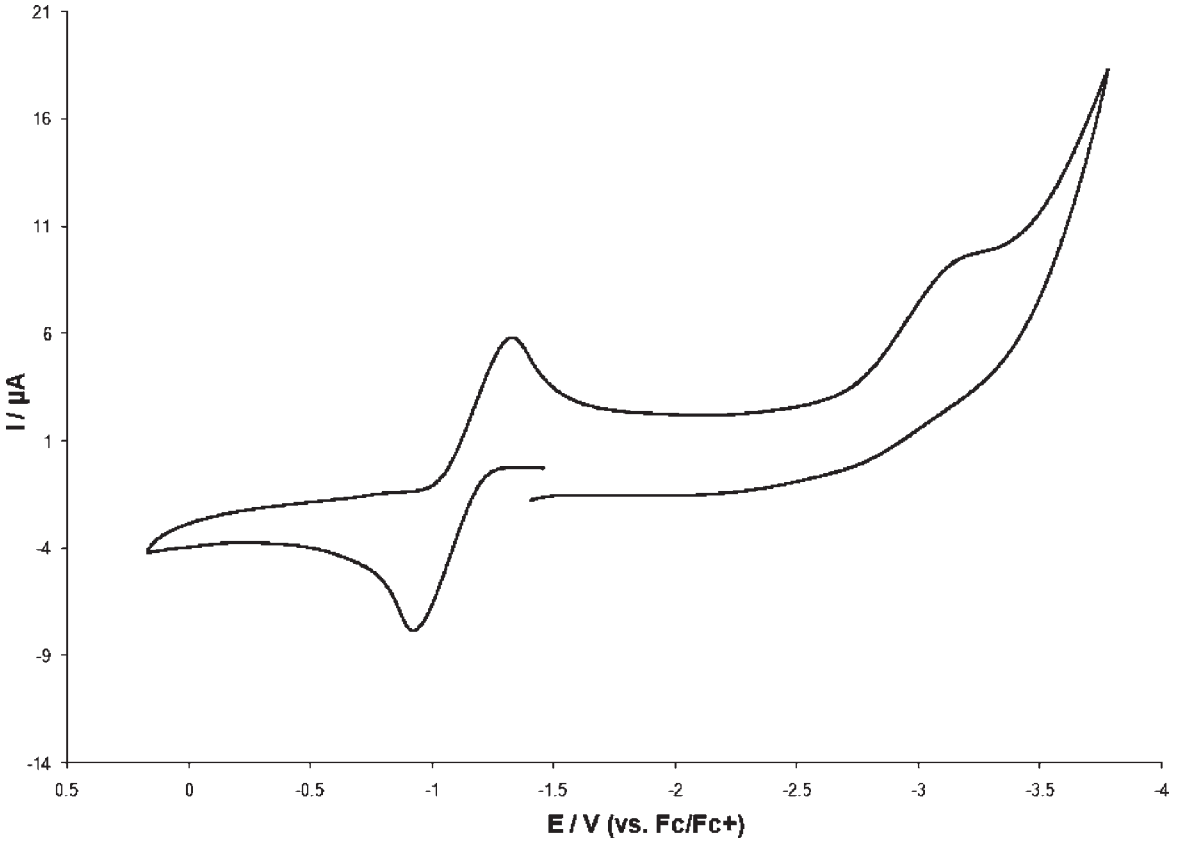

Figure 6. Room temperature cyclic voltammogram of **1** in THF vs $[Cp_2Fe]^{0/+}$ (Scan rate 0.2 V/s; 0.1 M $[NBu_4][PF_6]$ as supporting electrolyte.).

Scheme 2

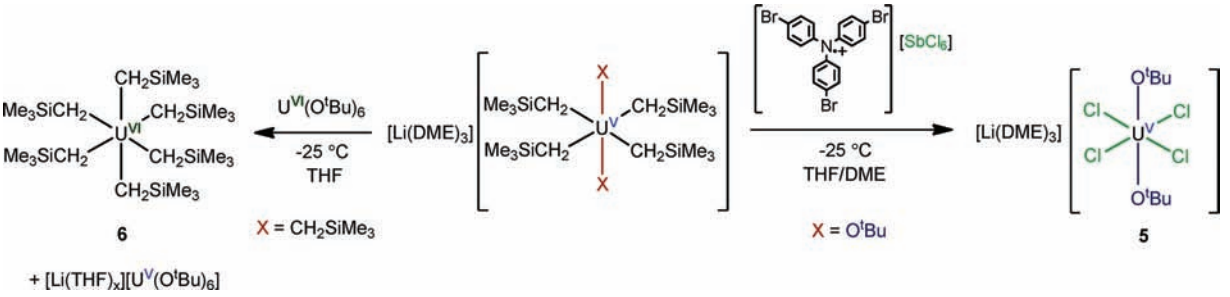

oxidants, such as the triarylaminium radical cations $[NAr_3]^+$.[58] Addition of 1 equiv of $[N(C_6H_4Br)_3][SbCl_6]$ to **1** in THF at −25 °C results in the formation of an intractable reaction mixture. In contrast, treatment of a cold solution of **4** in THF with 1 equiv of $[N(C_6H_4Br)_3][SbCl_6]$ results in the immediate formation of a near colorless solution. Removal of the solvent and recrystallization from DME affords pale green crystals of the U(V) complex $[Li(DME)_3][U(O^tBu)_2Cl_4]$ (**5**) in 48% yield (Scheme 2). Complex **5** was fully characterized, including analysis by X-ray crystallography (Figure S32, SI). It is likely formed by alkyl for chloride transmetalation, demonstrating the decidedly "non-innocent" behavior of the $[SbCl_6]^-$ counterion. Indeed, $[SbCl_6]^-$ is a known source of chloride ions.[58,87] The formation of **5** also highlights the sensitivity of the $U-C_{alkyl}$ bonds and further underlies the difficulty of generating a U(VI) complex possessing a uranium−carbon bond.

We have also explored the oxidation of **1** and **4** with several other common outer-sphere oxidants. However, the use of these alternate reagents was complicated by a variety of factors. For instance, neither $[Cp_2Fe][PF_6]$ nor $[Cp_2Fe][BPh_4]$ could be used because of their insolubility in cold THF, while reaction of **1** or **4** with $[CPh_3][PF_6]$ resulted in formation of intractable mixtures. As a result, we have pursued the use of $U(O^tBu)_6$ as an "innocent" oxidant, given the ample precedent of other outer-sphere homometallic electron transfers.[88−92] $U(O^tBu)_6$ has several attributes which make it ideal for the proposed transformation. It is both sterically saturated and highly soluble in both aliphatic and ethereal solvents.[48] Additionally, the product of its one-electron reduction, $[Li][U(O^tBu)_6]$, is readily identifiable by ^1H NMR spectroscopy.[48] On the basis of our electrochemical analysis, $U(O^tBu)_6$ is anticipated to behave as a mild oxidant toward both **1** and **4**. For instance, its reduction potential ($E_{1/2} = -1.12$ V vs $[Cp_2Fe]^{0/+}$)[48]

is only 100 mV greater than that found for **1** ($E_{1/2}$ = −1.22 V vs $[Cp_2Fe]^{0/+}$). Thus, addition of 1 equiv of $U(O^tBu)_6$ to **1** in THF-d_8 at −25 °C results in a rapid color change, to afford a deep-gold solution. The ^{1}H NMR spectrum of the resulting reaction mixture at −40 °C reveals the near total disappearance of **1** in solution, as well as the formation of two new resonances within the diamagnetic region at −3.15 ppm and 0.52 ppm in a 2:9 ratio, respectively (Figure S33, SI), assignable to the methyl and methylene resonances, respectively, of the homoleptic U(VI) alkyl complex $U(CH_2SiMe_3)_6$ (**6**). The ^{1}H NMR spectrum also displays a new resonance at 1.90 ppm corresponding to the methyl protons of $[Li(THF)_x][U(O^tBu)_6]$. Interestingly, at −40 °C this byproduct partially precipitates from the reaction mixture as colorless crystals. The formation of **6** in these solutions is further supported by the appearance of a resonance at 11.12 ppm in the $^{13}C\{^1H\}$ NMR spectrum, attributable to the methyl carbons of the methyltrimethylsilyl ligand of **6** (Figure S34, SI), while the ^{13}C resonance corresponding to the methylene carbons was observed indirectly, via an HMBC experiment, at 34.0 ppm (Figure S35, SI). Overall, these results strongly suggest that oxidation of **1** by $U(O^tBu)_6$ solely generates $U(CH_2SiMe_3)_6$ (**6**) and $[Li(THF)_x][U(O^tBu)_6]$ (Scheme 2). Furthermore, no evidence for alkyl ligand scrambling or α-elimination is observed by NMR spectroscopy. In this regard, it should be noted that attempts to prepare the analogous tungsten complex, by reaction of WCl_6 with $LiCH_2SiMe_3$, leads only to the formation of $(Me_3SiCH_2)_3W(\equiv CSiMe_3)$ in low yield.[93] Presumably, the smaller W^{6+} ion cannot support the steric bulk imposed by six methyltrimethylsilyl alkyl ligands, thereby promoting successive α-elimination reactions.

In contrast to the reaction with complex **1**, addition of 1 equiv of $U(O^tBu)_6$ to **4** in THF-d_8 at −25 °C results in no color change, while the ^{1}H NMR spectrum of the reaction mixture at −40 °C consists mostly of unreacted **4**. However, small amounts of $[Li(THF)_x][U(O^tBu)_6]$ and $SiMe_4$ are observed in the reaction mixture, while no unreacted $U(O^tBu)_6$ remains, suggesting that electron transfer is occurring, but that the resulting product is unstable, in line with conclusions drawn from the electrochemistry.

We have attempted to isolate complex **6** from its reaction mixtures but our efforts have been frustrated by both its high solubility in aliphatic and ethereal solvents as well as its thermal instability. Monitoring the in situ formation of **6** by ^{1}H NMR spectroscopy reveals **6** to be stable for at least 14 h at −40 °C in THF-d_8. Upon warming above −25 °C, however, complex **6** rapidly decomposes, producing **1** and $SiMe_4$ as its main decomposition products.

DFT Analysis. To gain further insight into the electronic structure of **1** and **6**, a DFT analysis was performed at the B3LYP level of theory. Additionally, the previously reported tetravalent uranium alkyl complex, $[U(CH_2SiMe_3)_5]^-$,[44] was also analyzed to compare with **1** and **6**. In $[U(CH_2SiMe_3)_5]^-$, the HOMO and HOMO−1 house the two unpaired electrons, and are predominantly 5f in character and nonbonding. The five U−C σ-interactions are located in HOMO−2 through to HOMO−6 (Table 1). Due to the D_{3h} symmetry, significant orbital mixing is observed, and several uranium-based orbitals contribute to each molecular orbital. Nonetheless, the 6d-orbitals are favored for U−C bonding (HOMO−3, HOMO−4, and HOMO−6), with only one U−C bond possessing significant 5f-orbital character (HOMO−2).

For complex **1**, the calculated geometry compares well with that observed experimentally. Specifically, the calculated U−C bond distances range from 2.443 Å to 2.472 Å, while those from the crystal structure range from 2.413(7) Å to 2.451(6) Å.

Table 1. Mulliken Populations and Orbital Energies for $[U^{IV}(CH_2SiMe_3)_5]^-$

orbital	energy (eV)	s	p	d	f	total	type
HOMO	−1.360	0.03	0.00	0.02	0.89	0.94	unpaired e^-
HOMO−1	−1.469	0.00	0.00	0.00	0.97	0.97	unpaired e^-
HOMO−2	−2.231	0.00	0.00	0.00	0.19	0.19	f_σ
HOMO−3	−2.286	0.00	0.00	0.12	0.05	0.17	d_σ
HOMO−4	−2.422	0.00	0.00	0.13	0.04	0.17	d_σ
HOMO−5	−3.320	0.06	0.00	0.09	0.07	0.22	$s_\sigma + d_\sigma + f_\sigma$
HOMO−6	−3.592	0.04	0.00	0.13	0.00	0.17	$s_\sigma + d_\sigma$

Additionally, the three largest calculated C−U−C angles range from 173.7° to 178.0°, which matches the experimentally observed structure. The Mulliken spin density of 1.45 is consistent with a U(V) complex having one unpaired 5f electron. This resides in the HOMO, which is predominantly metal based and nonbonding. The main orbitals involved in the uranium−carbon interactions are HOMO−1 through to HOMO−6, which constitute the six U−C σ interactions (Figure 7). According to the Mulliken population analysis, there is a substantial uranium contribution to all of the U−C σ interactions (Table 2). The three highest energy U−C bonding orbitals (HOMO−1, HOMO−2, and HOMO−3), which comprise the t_{1u} set, are nearly degenerate and exhibit ∼29% 5f-orbital participation. HOMO−4 (a_{1g} symmetry) exhibits 13% 7s-orbital participation, while the degenerate HOMO−5 and HOMO−6 orbitals (e_g symmetry) each exhibit 22% 6d-orbital participation. Notable is the nearly complete absence of 7p-orbital contribution to the six U−C bonding MOs (Table 2).

Complex **6** displays U−C bond lengths (2.353−2.377 Å) that are approximately 0.1 Å shorter than the distances observed in the pentavalent uranium complex, **1**. Additionally, DFT calculations predict a nearly octahedral geometry about the uranium center. For example, the three largest C−U−C angles range from 174.6° to 177.6°, as expected for an octahedron. Additionally, the nearly O_h geometry is likely the global minimum as a geometry optimization of complex **6** with C_{3v} symmetry converges to the previously observed octahedral structure. As observed with **1**, diamagnetic **6** exhibits six U−C σ interactions, which are found in the HOMO through to the HOMO−5 orbitals. The t_{1u} set (HOMO, HOMO−1, and HOMO−2) is nearly degenerate and exhibits ca. 35% 5f-orbital participation (Table 3), a somewhat higher f orbital participation that that observed for **1**. The HOMO−3 (a_{1g}) exhibits 10% 7s-orbital participation, while the degenerate e_g set (HOMO−4 and HOMO−5) exhibits 18% 6d-orbital participation. Interestingly, calculations on other U(VI) systems, including $[U(NR)_2]^{2+}$ and UH_6,[94,33] also reveal substantial amounts of f-orbital participation in metal ligand bonding.

Several features are of interest in the series comprising $[U(CH_2SiMe_3)_5]^-$, **1**, and **6** (Tables 1-3). Most importantly, the overall contribution of the 5f-orbitals increases with oxidation state. Specifically, the 5f contributions increase from 19% in U^{4+}, to 29% in U^{5+}, to 35% in U^{6+}. The relative amount of 6d and 7s contribution remains constant throughout the series indicating the 5f valence orbitals are taking a more dominant role in bonding upon increasing oxidation state. In all three complexes, the uranium contributions to the U−C bonding MOs are large, indicating strong covalent interactions, while the energy of the molecular orbitals drops expectedly with a higher effective

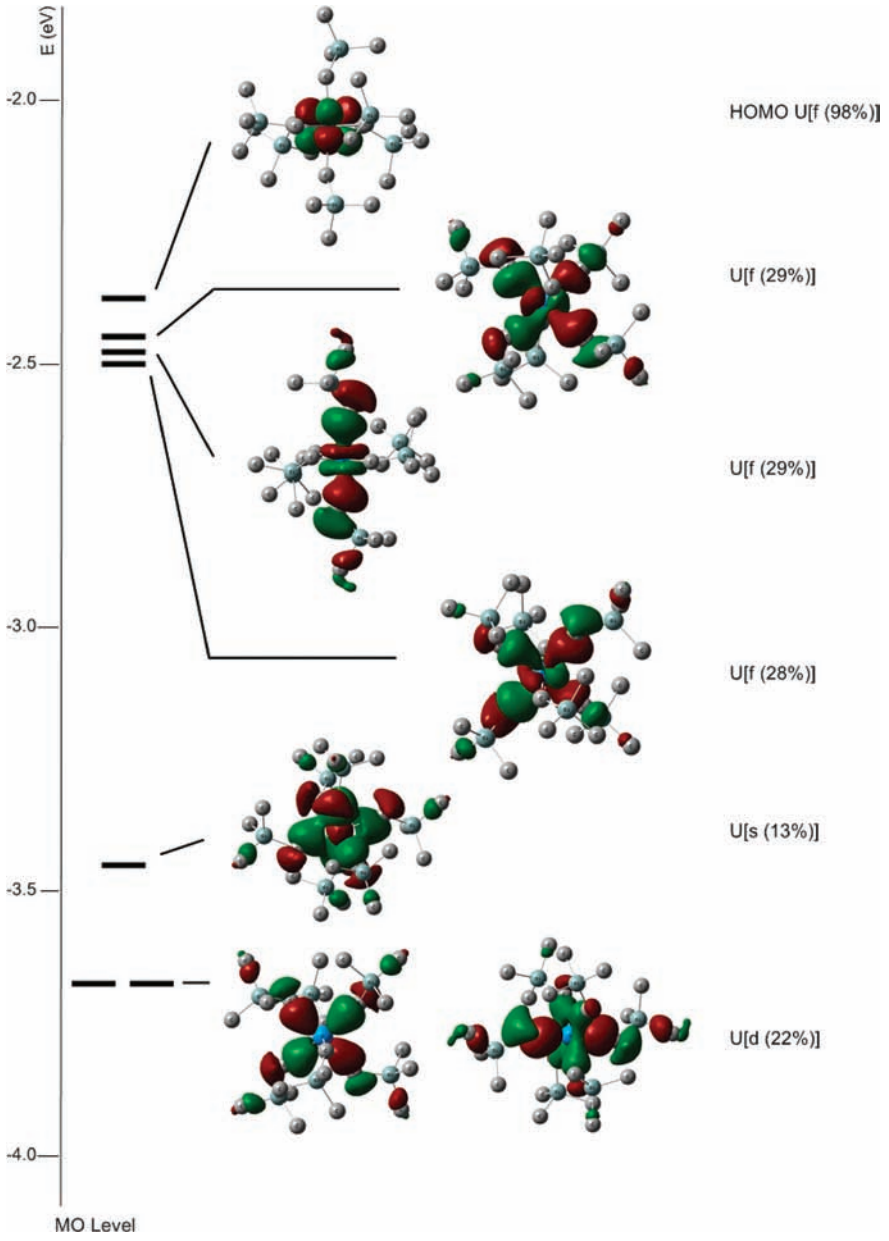

Figure 7. Highest occupied molecular orbitals for $[U(CH_2SiMe_3)_6]^-$ (**1**).

Table 2. Mulliken Populations and Orbital Energies for $[U^V(CH_2SiMe_3)_6]^-$ (1)

orbital	energy (eV)	s	p	d	f	total	type
HOMO	−2.367	0.00	0.00	0.00	0.98	0.98	unpaired e^-
HOMO−1	−2.449	0.00	0.01	0.00	0.29	0.30	f_σ
HOMO−2	−2.476	0.00	0.01	0.00	0.29	0.30	f_σ
HOMO−3	−2.503	0.00	0.01	0.00	0.28	0.29	f_σ
HOMO−4	−3.456	0.13	0.00	0.00	0.00	0.13	s_σ
HOMO−5	−3.673	0.00	0.00	0.22	0.00	0.22	d_σ
HOMO−6	−3.673	0.00	0.00	0.22	0.00	0.22	d_σ

Table 3. Mulliken Populations and Orbital Energies for $U^{VI}(CH_2SiMe_3)_6$ (6)

orbital	energy (eV)	s	p	d	f	total	type
HOMO	−5.850	0.00	0.00	0.00	0.35	0.35	f_σ
HOMO−1	−5.850	0.00	0.00	0.00	0.34	0.34	f_σ
HOMO−2	−5.905	0.00	0.00	0.00	0.35	0.35	f_σ
HOMO−3	−6.667	0.10	0.00	0.00	0.00	0.10	s_σ
HOMO−4	−7.102	0.00	0.00	0.18	0.00	0.18	d_σ
HOMO−5	−7.102	0.00	0.00	0.18	0.00	0.18	d_σ

nuclear charge. Given the above analysis, the difference in structural preference between the transition metals and actinide $[MR_6]^n$ complexes can be attributed to the surprising ability of complexes **1** and **6** to engage their f-orbitals in bonding. The *ungerade* character of the 5f-orbitals, like the *ungerade* p-orbitals of the main group elements, enforces an octahedral geometry for hexa-coordinate complexes,[10,33,95,96] and can potentially explain the octahedral structure observed for **1** and the octahedral structure predicted for **6**.

SUMMARY

Oxidation of $[Li(DME)_3][U(CH_2SiMe_3)_5]$ results in isolation of the unprecedented U(V) homoleptic alkyl complex $[Li(THF)_4][U(CH_2SiMe_3)_6]$. Similarly, oxidation of $[Li(DME)_3][U(O^tBu)_2(CH_2SiMe_3)_3]$ generates a mixed ligand U(V) alkyl/alkoxide complex, $[Li(DME)_3][U(O^tBu)_2(CH_2SiMe_3)_4]$. Both complexes exhibit octahedral geometries in the solid-state, while their thermal stabilities are enhanced by the steric saturation of the uranium metal center via 'ate' complex formation. Further oxidation to U(VI) is possible in the case of $[Li(THF)_4][U(CH_2SiMe_3)_6]$, resulting in the formation of $U(CH_2SiMe_3)_6$, which is only stable below −25 °C and could not be isolated. DFT calculations performed on $[Li(THF)_4][U(CH_2SiMe_3)_6]$ and $U(CH_2SiMe_3)_6$ reveal a surprising amount of 5f-orbital contribution to the U−C bonding MOs. Overall, the isolation of these high-valent complexes, in combination with the theoretical analysis, suggests that uranium can exhibit strongly covalent metal−ligand interactions and, given the correct ligand set, can form complexes that are "transition metal-like" in appearance.

EXPERIMENTAL SECTION

General. All reactions and subsequent manipulations were performed under anaerobic and anhydrous conditions either under a high vacuum or an atmosphere of argon or nitrogen. Diethyl ether, hexanes and THF were dried using a Vacuum Atmospheres DRI-SOLV solvent purification system. DME was distilled from sodium benzophenone ketyl. Pentane was dried over activated 4 Å for 24 h prior to use. All deuterated solvents were purchased from Cambridge Isotope Laboratories Inc. and were dried over activated 4 Å molecular sieves for 24 h prior to use. $[Li(DME)_3]U(CH_2SiMe_3)_5]$[44] and $U(O^tBu)_6$[48] were synthesized according to the published procedures. $LiCH_2SiMe_3$ was purchased from Sigma-Aldrich as a 1.0 M solution in pentane. Storage of the solution at −25 °C resulted in the deposition of $LiCH_2SiMe_3$ as a crystalline solid which was collected and dried in vacuo prior to use. All other reagents were obtained from commercial sources and used as received.

NMR spectra were recorded on a Varian UNITY INOVA 500 MHz spectrometer or a Bruker Avance III Ultrashield Plus 800 MHz spectrometer. ^1H and $^{13}C\{^1H\}$ NMR spectra were referenced to external $SiMe_4$. $^7Li\{^1H\}$ NMR spectra were referenced to an external saturated solution of LiCl in deuterium oxide. Elemental analyses were performed by the Micro-Mass Facility at the University of California, Berkeley. UV−vis/NIR spectra were recorded on a UV-3600 Shimadzu spectrophotometer.

Cyclic Voltammetry Measurements. Cyclic voltammetry (CV) experiments were performed using a CH Instruments 600c potentiostat, and the data were processed using CHI software (version 6.29). All experiments were performed in a glovebox using a 20-mL glass vial as the cell. The working electrode consisted of a platinum disk embedded in glass (2 mm diameter), and both the counter and reference electrodes consisted of platinum wire. Solutions employed during CV studies were typically 1 mM in the uranium complex and 0.1 M in $[Bu_4N][PF_6]$. All potentials are reported versus the $[Cp_2Fe]^{0/+}$ couple. For all trials, $i_{p,a}/i_{p,c} = 1$ for the $[Cp_2Fe]^{0/+}$ couple, while $i_{p,c}$ increased linearly with the square root of the scan rate (i.e., $\sqrt{v}$). Redox couples which exhibited behavior similar to that of the $[Cp_2Fe]^{0/+}$ couple were thus considered reversible.

Magnetism Measurements. Magnetism data were recorded using a Quantum Design MPMS 5XL SQUID magnetometer. All experiments were performed between 4 and 300 K using 50−100 mg of powdered, crystalline solid. Complexes **1**−**4** were loaded into an NMR tube, which was subsequently flame-sealed. The solid was kept in place with approximately 75 mg quartz wool packed on either side of the sample. The data were corrected for the contribution of the NMR tube and quartz wool. The experiments for **1**, **2** and **4** were performed using a 0.5 T field, whereas the experiment for **3** was performed using a 1 T field. Diamagnetic corrections ($\chi_{dia} = -6.50 \times 10^{-4}$ cm^3·mol^{-1} for **1**, $\chi_{dia} = -5.41 \times 10^{-4}$ cm^3·mol^{-1} for **2**, $\chi_{dia} = -4.34 \times 10^{-4}$ cm^3·mol^{-1} for **3**, $\chi_{dia} = -6.01 \times 10^{-4}$ cm^3·mol^{-1} for **4**) were made using Pascal's constants.[97]

*[Li(THF)$_4$][U(CH$_2$SiMe$_3$)$_6$] (**1**).* To a cold (−25 °C), stirring solution of $[Li(DME)_3][U(CH_2SiMe_3)_5]$ (0.306 g, 0.32 mmol) in Et_2O (8 mL) was added a solution of I_2 (0.041 g, 0.16 mmol) in Et_2O (2 mL) dropwise. This resulted in an immediate color change from green to dark red. The reaction mixture was stirred for 2 min, whereupon a solution of $LiCH_2SiMe_3$ (0.031 mg, 0.32 mmol) in Et_2O (6 mL) was added dropwise, causing the solution to turn deep green. The reaction mixture was then stirred for an additional 5 min, after which the solvent was removed in vacuo, affording a deep-green solid. The solid was subsequently dissolved in Et_2O (4 mL) and THF (1 mL) and filtered through a Celite column (2 cm × 0.5 cm) supported on glass wool. The filtrate was layered with hexanes (10 mL) and stored at −25 °C for 24 h, resulting in the formation of deep-green crystals. The crystals were washed with hexanes (2 × 2 mL) and dried under vacuum. 0.278 g, 82% yield. Crystals of **1** turn opaque upon application of vacuum. ^1H NMR (500 MHz, 25 °C, THF-d_8): δ −8.19 (s, 12H, CH_2SiMe_3), 0.86 (s, 54H, CH_2SiMe_3). $^{13}C\{^1H\}$ (201 MHz, 25 °C, THF-d_8): δ 42.15 (CH_2SiMe_3), CH_2SiMe_3 methylene resonance not observed. $^7Li\{^1H\}$ NMR (194 MHz, 25 °C, THF-d_8): δ 3.22 (s). Anal. Calcd for $C_{40}H_{98}LiO_4Si_6U$: C, 45.47; H, 9.35. Found: C, 44.58; H, 8.86. UV−vis/NIR (THF, 14.0 mM, 25 °C, L·mol^{-1}·cm^{-1}): 870 (sh, ε = 11.4), 948 (sh, ε = 7.5), 1028 (ε = 3.9), 1088 (ε = 3.0), 1191 (ε = 2.2), 1222 (sh, ε = 1.9), 1301 (ε = 2.0), 1323 (sh, ε = 1.9), 1385 (ε = 2.5), 1462 (ε = 5.8), 1522 (ε = 2.3).

*[Li(DME)$_3$][U(O^{t}Bu)$_2$(CH$_2$SiMe$_3$)$_3$] (**2**).* To a stirring solution of $[Li(DME)_3][U(CH_2SiMe_3)_5]$ (1.001 g, 1.05 mmol) in DME (6 mL) was added *tert*-butanol (0.156 g, 2.10 mmol). The reaction mixture was stirred for 5 h resulting in the formation of a pink solution concomitant with the deposition of pink, crystalline solid. Storage of this solution at −25 °C for 24 h resulted in the further deposition of pink crystalline material. The crystals were washed with Et_2O (2 × 2 mL) and dried under vacuum. 0.835 g, 86% yield. ^1H NMR (500 MHz, 25 °C, THF-d_8): δ −229.29 (s, 6H, CH_2SiMe_3), −33.28 (s, 27H, CH_2SiMe_3), 3.33 (s, 18H, DME), 3.48 (s, 12H, DME), 90.37 (s, 18H, CCH_3). $^7Li\{^1H\}$ NMR (194 MHz, 25 °C, THF-d_8): δ 1.20 (s). Anal. Calcd for $C_{32}H_{81}LiO_8Si_3U$: C, 41.63; H, 8.84. Found: C, 41.74; H, 8.82. UV−vis/NIR (DME, 8.89 mM, 25 °C, L·mol^{-1}·cm^{-1}): 422 (ε = 43.0), 454 (ε = 59.4), 492 (sh, ε = 10.9), 512 (ε = 17.8), 546 (ε = 32.3), 586 (ε = 39.0), 662 (ε = 3.3), 712 (ε = 3.9), 758 (ε = 9.7), 820 (sh, ε = 24.6), 854 (ε = 36.8), 954 (ε = 26.2), 1006 (ε = 9.9), 1062 (ε = 42.8), 1168 (ε = 30.5), 1380 (ε = 50.0), 1416 (ε = 44.3), 1490 (ε = 76.8).

*(Me$_3$SiCH$_2$)Ag(μ-CH$_2$SiMe$_3$)U(CH$_2$SiMe$_3$)(O^{t}Bu)$_2$(DME) (**3**).* To a cold (−25 °C), stirring suspension of **2** (0.103 g, 0.11 mmol) in Et_2O (8 mL) was added a suspension of AgOTf (0.029 g, 0.11 mmol) in Et_2O (2 mL). Upon addition, the reaction mixture immediately lightened to give a pale-yellow solution. After 5 min, the solvent was removed in vacuo to give a tacky pink solid. The solid was dissolved into cold pentane (4 mL, −25 °C) and filtered through a Celite column (2 cm × 0.5 cm) supported on glass wool. Storage of the solution at −25 °C for 24 h resulted in the formation of pink blocks. 0.060 mg, 64% yield. ^1H NMR (500 MHz, 25 °C, C_7D_8): δ −63.04 (s, 6H, DME), −54.48 (s, 4H, DME), −24.13 (s, 2H, CH_2SiMe_3), −18.95 (s, 9H, CH_2SiMe_3), −15.71 (s, 18H, CH_2SiMe_3), 86.62 (s, 18H, CCH_3), resonances corresponding to two CH_2SiMe_3 groups were not observed. Anal. Calcd for $C_{24}H_{61}AgO_4Si_3U$: C, 34.15; H, 7.30. Found: C, 34.36; H, 7.53. UV−vis/NIR (DME, 7.48 mM, 25 °C, L·mol^{-1}·cm^{-1}): 422 (ε = 30.2), 462 (ε = 22.9), 498 (sh, ε = 12.6), 514 (ε = 14.1), 570 (ε = 17.3), 592 (ε = 11.5), 644 (ε = 7.5), 698 (ε = 4.7), 754 (sh, ε = 10.0), 826 (ε = 22.9), 924 (ε = 13.8), 1014 (ε = 13.7), 1036 (ε = 19.5), 1116 (ε = 52.1), 1162 (ε = 44.0), 1250 (ε = 7.8), 1372 (ε = 34.4), 1498 (ε = 27.9).

Table 4. X-ray Crystallographic Data for Complexes 1, 2, 3, 4·Et_2O, and 5

	1	2	3	4·Et_2O	5
empirical formula	$C_{40}H_{98}LiO_4Si_6U$	$C_{32}H_{81}LiO_8Si_3U$	$C_{24}H_{61}AgO_4Si_3U$	$C_{36}H_{92}LiO_8Si_4U\cdot Et_2O$	$C_{20}H_{48}Cl_4LiO_8U$
crystal habit, color	plate, dark green	plate, pink	block, pink	block, dark red	irregular, pale green
crystal size (mm^3)	0.55 × 0.55 × 0.12	0.7 × 0.7 × 0.07	0.9 × 0.8 × 0.8	1.0 × 0.6 × 0.4	0.9 × 0.6 × 0.25
crystal system	monoclinic	trigonal	monoclinic	tetragonal	monoclinic
space group	$P2_1/c$	$P\bar{3}1c$	$P2_1/n$	$P4_2/mmc$	$P2_1/c$
volume ($Å^3$)	5764.3(6)	2383.2(7)	3678(1)	2981.8(3)	3320.2(8)
a (Å)	22.313(1)	13.059(2)	14.946(2)	12.3874(4)	11.053(2)
b (Å)	13.3374(8)	13.059(2)	16.125(3)	12.3874(4)	15.790(2)
c (Å)	19.370(1)	16.136(4)	15.267(2)	19.432(1)	19.038(3)
α (deg)	90	90	90	90	90
β (deg)	90.352(2)	90	91.738(2)	90	92.248(2)
γ (deg)	90	120	90	90	90
Z	2	2	4	2	4
formula weight (g/mol)	1056.82	923.26	843.95	1084.62	803.34
density (calculated) (Mg/m^3)	1.204	1.229	1.524	1.177	1.607
absorption coefficient (mm^{-1})	2.970	3.515	5.050	2.840	5.245
F_{000}	2148	866	1672	1074	1580
total no. reflections	46869	16705	30428	23433	27237
unique reflections	11646	1757	7740	1836	6769
final R indices [$I > 2\sigma(I)$]	R_1 = 0.0456, wR_2 = 0.1196	R_1 = 0.0355, wR_2 = 0.1002	R_1 = 0.0411, wR_2 = 0.1026	R_1 = 0.0392, wR_2 = 0.0973	R_1 = 0.0350, wR_2 = 0.0856
Largest diff. peak and hole ($e^-Å^{-3}$)	1.936 and −1.296	1.175 and −0.963	2.780 and −2.081	0.767 and −1.039	1.015 and −2.442
GOF	0.924	1.308	0.989	1.177	1.001

*[Li(DME)$_3$][U(O^{t}Bu)$_2$(CH$_2$SiMe$_3$)$_4$] (**4**).* To a cold (−25 °C), stirring suspension of **2** (0.403 g, 0.44 mmol) in DME (6 mL) was added Me_3NO (0.018 g, 0.24 mmol). Upon addition, the reaction immediately turned dark red. The reaction mixture was stirred for 15 min, after which the solvent was removed in vacuo, affording a deep-red solid. The solid was washed with hexanes (3 × 2 mL) and dried in vacuo. The resulting material was subsequently dissolved in Et_2O (6 mL) and filtered through a Celite column (2 cm × 0.5 cm) supported on glass wool. The filtrate was layered with hexanes (8 mL) and stored at −25 °C for 24 h, resulting in the formation of deep-red crystals. The crystals were washed with hexanes (2 × 2 mL) and dried under vacuum. 0.191 g, 43% yield. Crystals of **4** turn opaque upon application of vacuum. ^{1}H NMR (500 MHz, 25 °C, THF-d_8): δ −0.79 (s, 36H, CH_2SiMe_3), −0.38 (s, 8H, CH_2SiMe_3), 3.28 (s, 18H, DME), 3.44 (s, 12H, DME), 7.37 (s, 18H, CCH_3). ^{7}Li{^{1}H} NMR (194 MHz, 25 °C, THF-d_8): δ 3.09 (s). Anal. Calcd $C_{36}H_{92}LiO_8Si_4U$: C, 42.78; H, 9.19. Found: C, 42.30; H, 9.22.

*[Li(DME)$_3$][U(O^{t}Bu)$_2$Cl$_4$] (**5**).* To a cold (−25 °C) stirring suspension of **4** (0.085 g, 0.08 mmol) in THF (4 mL) was added a solution of [N(C$_6$H$_4$Br)$_3$][SbCl$_6$] (0.067 g, 0.08 mmol) in THF (4 mL). Upon addition, the reaction immediately turned pale green. The reaction mixture was stirred for 15 min, after which the solvent was removed in vacuo affording a pale-green solid. The solid was washed with Et_2O (3 × 2 mL) and dried in vacuo. The resulting material was subsequently dissolved in DME (3 mL) and filtered through a Celite column (2 cm × 0.5 cm) supported on glass wool. Storage of the solution at −25 °C for 1 week, resulted in the formation of pale-green crystals. The crystals were washed with hexanes (2 × 2 mL) and dried under vacuum. 0.033 g, 49% yield. Crystals of **6** turn opaque upon application of vacuum. ^{1}H NMR (500 MHz, 25 °C, C_6D_6): δ 2.80 (s, 30H, DME), 4.24 (s, 6H, CCH_3, cis isomer), 5.21 (s, 12H, CCH_3, trans isomer). ^{7}Li{^{1}H} NMR (194 MHz, 25 °C, THF-d_8): δ −2.00 (s). Anal. Calcd for $C_{20}H_{48}Cl_4LiO_8U$: C, 29.90; H, 6.02. Found: C, 29.57; H, 6.00. UV−vis/NIR (DME, 9.38 mM, 25 °C, L·mol^{-1}·cm^{-1}): 656 (ε = 2.7), 808 (ε = 2.9), 858 (ε = 4.9), 932 (ε = 1.0), 1014 (ε = 1.2), 1064 (ε = 2.1), 1464 (ε = 1.9), 1542 (ε = 4.4), 1626 (ε = 3.0).

*U(CH$_2$SiMe$_3$)$_6$ (**6**).* An NMR tube equipped with a J-Young valve was charged with a cold (−25 °C) deep-red solution of U(O^{t}Bu)$_6$ (0.034 g, 0.050 mmol) in THF-d_8 (0.3 mL). To this was added a cold (−25 °C) deep-green solution of **1** (0.054 g, 0.051 mmol) in THF-d_8 (0.3 mL). Upon addition, the reaction mixture immediately turned deep gold in color. The NMR tube was subsequently placed on CO_2(s) and transported to an NMR spectrometer precooled to −40 °C. Upon standing at −40 °C, a colorless, crystalline material formed, indicating the precipitation of [Li(THF)$_x$][U(O^{t}Bu)$_6$] from the reaction mixture. ^{1}H NMR (500 MHz, −40 °C, THF-d_8): δ −3.15 (s, 12H, CH_2SiMe_3), 0.52 (s, 54H, CH_2SiMe_3). ^{13}C{^{1}H} (125 MHz, −40 °C, THF-d_8): δ 11.12 (CH_2SiMe_3), CH_2SiMe_3 methylene resonance not observed. HMBC (125 MHz, −40 °C, THF-d_8): δ 9.0 (CH_2SiMe_3), 30.4 (CH_2SiMe_3).

Warming the reaction mixture to room temperature resulted in the rapid disappearance of the resonances assigned to **6** and the formation of **1** and $SiMe_4$. Recooling the solution to −40 °C left the resonances assigned to **1** and [Li(THF)$_x$][U(O^{t}Bu)$_6$] unchanged (see Supporting Information).

Reaction of 4 with U(O^{t}Bu)$_6$. An NMR tube equipped with a J-Young valve was charged with a cold (−25 °C) deep-red solution of U(O^{t}Bu)$_6$ (0.015 g, 0.022 mmol) in THF-d_8 (0.3 mL). To this was added a cold (−25 °C) deep-red solution of **4** (0.023 g, 0.023 mmol) in THF-d_8 (0.3 mL). The NMR tube was subsequently placed on CO_2(s) and transported to an NMR spectrometer precooled to −40 °C. The deep-red reaction mixture was examined by ^{1}H NMR spectroscopy, revealing the presence of **4**, [Li(THF)$_x$][U(O^{t}Bu)$_6$], and $SiMe_4$ in solution (Figure S38, SI).

X-ray Crystallography. Data for **1**−**5** were collected on a Bruker 3-axis platform diffractometer equipped with a SMART-1000 CCD detector using a graphite monochromator with a Mo Kα X-ray source (α = 0.71073 Å). The crystals were mounted on a glass fiber under Paratone-N oil, and all data were collected at 150(2) K using an Oxford nitrogen gas cryostream system. A hemisphere of data was collected using ω scans with 0.3° frame widths. Frame exposures of 10, 15, 7, 5, and 10 s were used for **1**, **2**, **3**, **4**·Et_2O, and **5**, respectively.

Data collection and cell parameter determination were conducted using the SMART program. [98] Integration of the data frames and final cell parameter refinement were performed using SAINT software.[99] Absorption correction of the data was carried out empirically based on reflection ψ-scans. Subsequent calculations were carried out using SHELXTL.[100] Structure determination was done using direct or Patterson methods and difference Fourier techniques. All hydrogen atom positions were idealized and rode on the atom of attachment with exceptions noted in the subsequent paragraph. Structure solution, refinement, graphics, and creation of publication materials were performed using SHELXTL.[100]

One of the two $[U(CH_2SiMe_3)_6]^-$ fragments in complex **1** was disordered over two orientations, in a 67:33 ratio. As a result, each of the three crystallographically unique methyltrimethysilyl ligands was modeled in two positions. The $[Li(DME)_3]^+$ cation in complex **2** was disordered over two orientations in a 50:50 ratio. Within the cation, the C−C bond distances were fixed at 1.45(1) Å, while the closest neighboring carbon atom distances were fixed at 2.60(1) Å, both using the DFIX command. In addition, the methyltrimethysilyl ligand in **2** was disordered over two orientations, also in a 50:50 ratio. For complex **3**, one butoxide ligand was found to be disordered between two positions about the tertiary carbon atom, in a 50:50 ratio. Within the butoxide moiety, the closest neighboring carbon atom distances were fixed at 1.4(1) Å, using the DFIX command, while the carbon atoms were further restrained using FLAT and EADP. Both the $[Li(DME)_3]^+$ cation and the Et_2O solvate molecule in complex **4** were disordered. Within the $[Li(DME)_3]^+$ cation, the C−C and C−O bond distances were fixed at 1.5(1) Å and 1.4(1) Å, respectively, while the closest neighboring oxygen atom distances were fixed at 2.0(1) Å using the DFIX command. Each of these disordered moieties was modeled over two orientations in a 50:50 ratio. In addition, the butoxide ligand was found to be disordered between two positions about the tertiary carbon atom, in a 50:50 ratio, while the crystallographically unique methyltrimethysilyl ligand was also disordered over two orientations in a 50:50 ratio. For all structures, idealized hydrogen atoms were not assigned to the disordered carbon atoms. A summary of relevant crystallographic data for **1**, **2**, **3**, **4**·Et_2O, and **5** is presented in Table 4.

Computational Details. The electronic structures of $[U(CH_2SiMe_3)_5]^-$, **1**, and **6** were examined using the *Gaussian09* software program[101] at the B3LYP[102,103] level using the Stuttgart basis set, while the corresponding effective core potential was used for U. The most diffuse s, p, d, and f functions were removed, leaving 7s/6p/5d/3f. The 6-31G(d′) basis set[104] was used for C, H, and Si. The optimized structures of **1** and **6** were confirmed to be minima by harmonic vibrational frequency calculations with no imaginary frequencies found. For $[U(CH_2SiMe_3)_5]^{1-}$, the crystal structure coordinates were used and a single-point calculation was done. Mulliken population analyses on all three compounds were performed to determine orbital involvement.

■ ASSOCIATED CONTENT

Supporting Information. X-ray crystallographic details (as CIF files), magnetic susceptibility plots, tabulated cyclic voltammetry data, and spectral data for **1**−**5**. Complete version of reference 101. This material is available free of charge via the Internet at http://pubs.acs.org.

■ AUTHOR INFORMATION

Corresponding Author
hayton@chem.ucsb.edu

■ ACKNOWLEDGMENT

We thank the University of California, Santa Barbara and the Department of Energy (BES Heavy Element Program) for financial support of this work. We also thank Dr. Hongjun Zhou for his assistance with the HMBC experiments. J.R.W. gratefully acknowledges the University of Missouri and the U.S. Department of Homeland Security's National Technical Nuclear Forensics Center for support.

■ REFERENCES

(1) Demolliens, A.; Jean, Y.; Eisenstein, O. *Organometallics* **1986**, *5*, 1457–1464.
(2) Kang, S. K.; Albright, T. A.; Eisenstein, O. *Inorg. Chem.* **1989**, *28*, 1611–1613.
(3) Kang, S. K.; Tang, H.; Albright, T. A. *J. Am. Chem. Soc.* **1993**, *115*, 1971–1981.
(4) Tanpipat, N.; Baker, J. *J. Phys. Chem.* **1996**, *100*, 19818–19823.
(5) Kaupp, M. *J. Am. Chem. Soc.* **1996**, *118*, 3018–3024.
(6) Kaupp, M. *Chem.—Eur. J.* **1998**, *4*, 1678–1686.
(7) Kaupp, M. *Angew. Chem., Int. Ed.* **2001**, *40*, 3534–3565.
(8) Pfennig, V.; Seppelt, K. *Science* **1996**, *271*, 626–628.
(9) Kleinhenz, S.; Pfennig, V.; Seppelt, K. *Chem.—Eur. J.* **1998**, *4*, 1687–1691.
(10) Seppelt, K. *Acc. Chem. Res.* **2003**, *36*, 147–153.
(11) Morse, P. M.; Girolami, G. S. *J. Am. Chem. Soc.* **1989**, *111*, 4114–4116.
(12) Landis, C. R.; Cleveland, T.; Firman, T. K. *J. Am. Chem. Soc.* **1995**, *117*, 1859–1860.
(13) Landis, C. R.; Firman, T. K.; Root, D. M.; Cleveland, T. *J. Am. Chem. Soc.* **1998**, *120*, 1842–1854.
(14) Landis, C. R.; Cleveland, T.; Firman, T. K. *J. Am. Chem. Soc.* **1998**, *120*, 2641–2649.
(15) Cameron, A. D.; Fitzgerald, G.; Zerner, M. C. *Inorg. Chem.* **1988**, *27*, 3437–3439.
(16) Jonas, V.; Frenking, G.; Gauss, J. *Chem. Phys. Lett.* **1992**, *194*, 109–117.
(17) McGrady, G. S.; Downs, A. J. *Coord. Chem. Rev.* **2000**, *197*, 95–124.
(18) Shortland, A. J.; Wilkinson, G. *J. Chem. Soc., Dalton Trans.* **1973**, 872–876.
(19) Galyer, A. L.; Wilkinson, G. *J. Chem. Soc., Dalton Trans.* **1976**, 2235–2238.
(20) Vaid, T. P.; Veige, A. S.; Lobkovsky, E. B.; Glassey, W. V.; Wolczanski, P. T.; Liable-Sands, L. M.; Rheingold, A. L.; Cundari, T. R. *J. Am. Chem. Soc.* **1998**, *120*, 10067–10079.
(21) Denning, R. *Struct. Bonding (Berlin)* **1992**, *79*, 215–276.
(22) Denning, R. G. *J. Phys. Chem. A* **2007**, *111*, 4125–4143.
(23) Denning, R. G.; Green, J. C.; Hutchings, T. E.; Dallera, C.; Tagliaferri, A.; Giarda, K.; Brookes, N. B.; Braicovich, L. *J. Chem. Phys.* **2002**, *117*, 8008–8021.
(24) Prodan, I. D.; Scuseria, G. E.; Martin, R. L. *Phys. Rev. B* **2007**, *76*, 033101.
(25) Walensky, J. R.; Martin, R. L.; Ziller, J. W.; Evans, W. J. *Inorg. Chem.* **2010**, *49*, 10007–10012.
(26) Kozimor, S. A.; Yang, P.; Batista, E. R.; Boland, K. S.; Burns, C. J.; Clark, D. L.; Conradson, S. D.; Martin, R. L.; Wilkerson, M. P.; Wolfsberg, L. E. *J. Am. Chem. Soc.* **2009**, *131*, 12125–12136.
(27) Arnold, P.; Turner, Z.; Kaltsoyannis, N.; Pelekanaki, P.; Bellabarba, R.; Tooze, R. *Chem.—Eur. J.* **2010**, *16*, 9623–9629.
(28) Raymond, K. N.; Eigenbrot, C. W. *Acc. Chem. Res.* **1980**, *13*, 276–283.
(29) Cantat, T.; Graves, C. R.; Jantunen, K. C.; Burns, C. J.; Scott, B. L.; Schelter, E. J.; Morris, D. E.; Hay, P. J.; Kiplinger, J. L. *J. Am. Chem. Soc.* **2008**, *130*, 17537–17551.
(30) Li, J.; Bursten, B. E. *J. Am. Chem. Soc.* **1997**, *119*, 9021–9032.
(31) Tassell, M. J.; Kaltsoyannis, N. *Dalton Trans.* **2010**, *39*, 6719–6725.
(32) Ingram, K. I. M.; Kaltsoyannis, N.; Gaunt, A. J.; Neu, M. P. *J. Alloys Compd.* **2007**, *444*−*445*, 369–375.

(33) Straka, M.; Hrobarik, P.; Kaupp, M. *J. Am. Chem. Soc.* **2005**, *127*, 2591–2599.
(34) Straka, M.; Patzschke, M.; Pyykko, P. *Theor. Chem. Acc.* **2003**, *109*, 332–340.
(35) Tourneux, J.-C.; Berthet, J.-C.; Cantat, T.; Thuery, P.; Mezailles, N.; Ephritikhine, M. *J. Am. Chem. Soc.* **2011**, *133*, 6162–6165.
(36) Graves, C. R.; Kiplinger, J. L. *Chem. Commun.* **2009**, 3831–3853.
(37) Sigurdson, E. R.; Wilkinson, G. *J. Chem. Soc., Dalton Trans.* **1977**, 812–818.
(38) Marks, T. J. *Prog. Inorg. Chem.* **1979**, *25*, 223–333.
(39) Korobkov, I.; Gambarotta, S. *Inorg. Chem.* **2010**, *49*, 3409–3418.
(40) Fortier, S.; Wu, G.; Hayton, T. W. *J. Am. Chem. Soc.* **2010**, *132*, 6888–6889.
(41) Graves, C. R.; Vaughn, A. E.; Schelter, E. J.; Scott, B. L.; Thompson, J. D.; Morris, D. E.; Kiplinger, J. L. *Inorg. Chem.* **2008**, *47*, 11879–11891.
(42) Graves, C. R.; Scott, B. L.; Morris, D. E.; Kiplinger, J. L. *Organometallics* **2008**, *27*, 3335–3337.
(43) Maynadié, J.; Barros, N.; Berthet, J.-C.; Thuéry, P.; Maron, L.; Ephritikhine, M. *Angew. Chem., Int. Ed.* **2007**, *46*, 2010–2012.
(44) Fortier, S.; Melot, B. C.; Wu, G.; Hayton, T. W. *J. Am. Chem. Soc.* **2009**, *131*, 15512–15521.
(45) Seaman, L. A.; Fortier, S.; Wu, G.; Hayton, T. W. *Inorg. Chem.* **2011**, *50*, 636–646.
(46) Davidson, P. J.; Lappert, M. F.; Pearce, R. *Acc. Chem. Res.* **1974**, *7*, 209–217.
(47) Davidson, P. J.; Lappert, M. F.; Pearce, R. *Chem. Rev.* **1976**, *76*, 219–242.
(48) Fortier, S.; Wu, G.; Hayton, T. W. *Inorg. Chem.* **2008**, *47*, 4752–4761.
(49) Song, L.; Trogler, W. C. *Angew. Chem., Int. Ed.* **1992**, *31*, 770–772.
(50) Ray, L.; Shaikh, M. M.; Ghosh, P. *Inorg. Chem.* **2007**, *47*, 230–240.
(51) Papasergio, R. I.; Raston, C. L.; White, A. H. *J. Chem. Soc., Dalton Trans.* **1987**, 3085–3091.
(52) Cordero, B.; Gomez, V.; Platero-Prats, A. E.; Reves, M.; Echeverria, J.; Cremades, E.; Barragan, F.; Alvarez, S. *Dalton Trans.* **2008**, 2832–2838.
(53) Pyykko, P. *Chem. Rev.* **1997**, *97*, 597–636.
(54) Rawashdeh-Omary, M. A.; Omary, M. A.; Patterson, H. H. *J. Am. Chem. Soc.* **2000**, *122*, 10371–10380.
(55) Moret, M.-E.; Chen, P. *J. Am. Chem. Soc.* **2009**, *131*, 5675–5690.
(56) Brumas-Soula, B.; Dahan, F.; Poilblanc, R. *New J. Chem.* **1998**, *22*, 1067–1074.
(57) Song, H.-B.; Zhang, Z.-Z.; Mak, T. C. W. *Inorg. Chem.* **2001**, *40*, 5928–5933.
(58) Connelly, N. G.; Geiger, W. E. *Chem. Rev.* **1996**, *96*, 877–910.
(59) Sternal, R. S.; Brock, C. P.; Marks, T. J. *J. Am. Chem. Soc.* **1985**, *107*, 8270–8272.
(60) Sternal, R. S.; Marks, T. J. *Organometallics* **1987**, *6*, 2621–2623.
(61) Gardner, B. M.; McMaster, J.; Lewis, W.; Liddle, S. T. *Chem. Commun.* **2009**, 2851–2853.
(62) Patel, D.; King, D. M.; Gardner, B. M.; McMaster, J.; Lewis, W.; Blake, A. J.; Liddle, S. T. *Chem. Commun.* **2010**, *47*, 295–297.
(63) Minasian, S. G.; Krinsky, J. L.; Williams, V. A.; Arnold, J. *J. Am. Chem. Soc.* **2008**, *130*, 10086–10087.
(64) Minasian, S. G.; Krinsky, J. L.; Rinehart, J. D.; Copping, R.; Tyliszczak, T.; Janousch, M.; Shuh, D. K.; Arnold, J. *J. Am. Chem. Soc.* **2009**, *131*, 13767–13783.
(65) Quadrelli, E. A.; Poli, R. *Organometallics* **1998**, *17*, 5776–5781.
(66) Lanci, M. P.; Remy, M. S.; Kaminsky, W.; Mayer, J. M.; Sanford, M. S. *J. Am. Chem. Soc.* **2009**, *131*, 15618–15620.
(67) Graves, C. R.; Yang, P.; Kozimor, S. A.; Vaughn, A. E.; Clark, D. L.; Conradson, S. D.; Schelter, E. J.; Scott, B. L.; Thompson, J. D.; Hay, P. J.; Morris, D. E.; Kiplinger, J. L. *J. Am. Chem. Soc.* **2008**, *130*, 5272–5285.
(68) Spencer, L. P.; Schelter, E. J.; Yang, P.; Gdula, R. L.; Scott, B. L.; Thompson, J. D.; Kiplinger, J. L.; Batista, E. R.; Boncella, J. M. *Angew. Chem., Int. Ed.* **2009**, *48*, 3795–3798.
(69) Castro-Rodriguez, I.; Olsen, K.; Gantzel, P.; Meyer, K. *J. Am. Chem. Soc.* **2003**, *125*, 4565–4571.
(70) Castro-Rodriguez, I.; Meyer, K. *Chem. Commun.* **2006**, 1353–1368.
(71) Bart, S. C.; Anthon, C.; Heinemann, F. W.; Bill, E.; Edelstein, N. M.; Meyer, K. *J. Am. Chem. Soc.* **2008**, *130*, 12536–12546.
(72) Castro-Rodriguez, I.; Nakai, H.; Meyer, K. *Angew. Chem., Int. Ed.* **2006**, *45*, 2389–2392.
(73) Rinehart, J. D.; Harris, T. D.; Kozimor, S. A.; Bartlett, B. M.; Long, J. R. *Inorg. Chem.* **2009**, *48*, 3382–3395.
(74) Schelter, E. J.; Yang, P.; Scott, B. L.; Thompson, J. D.; Martin, R. L.; Hay, P. J.; Morris, D. E.; Kiplinger, J. L. *Inorg. Chem.* **2007**, *46*, 7477–7488.
(75) Reynolds, J. G.; Zalkin, A.; Templeton, D. H.; Edelstein, N. M. *Inorg. Chem.* **1977**, *16*, 1090–1096.
(76) Stewart, J. L.; Andersen, R. A. *New J. Chem.* **1995**, *19*, 587–595.
(77) Schelter, E. J.; Veauthier, J. M.; Graves, C. R.; John, K. D.; Scott, B. L.; Thompson, J. D.; Pool-Davis-Tournear, J. A.; Morris, D. E.; Kiplinger, J. L. *Chem.—Eur. J.* **2008**, *14*, 7782–7790.
(78) Schelter, E. J.; Morris, D. E.; Scott, B. L.; Thompson, J. D.; Kiplinger, J. L. *Inorg. Chem.* **2007**, *46*, 5528–5536.
(79) Hutchison, C. A.; Elliot, N. *J. Chem. Phys.* **1948**, *16*, 920–927.
(80) Bart, S. C.; Heinemann, F. W.; Anthon, C.; Hauser, C.; Meyer, K. *Inorg. Chem.* **2009**, *48*, 9419–9426.
(81) Lam, O. P.; Bart, S. C.; Kameo, H.; Heinemann, F. W.; Meyer, K. *Chem. Commun.* **2010**, *46*, 3137–3139.
(82) Lam, O. P.; Anthon, C.; Heinemann, F. W.; O'Connor, J. M.; Meyer, K. *J. Am. Chem. Soc.* **2008**, *130*, 6567–6576.
(83) Lam, O. P.; Feng, P. L.; Heinemann, F. W.; O'Connor, J. M.; Meyer, K. *J. Am. Chem. Soc.* **2008**, *130*, 2806–2816.
(84) Kozimor, S. A.; Bartlett, B. M.; Rinehart, J. D.; Long, J. R. *J. Am. Chem. Soc.* **2007**, *129*, 10672–10674.
(85) Broderick, E. M.; Gutzwiller, N. P.; Diaconescu, P. L. *Organometallics* **2010**, *29*, 3242–3251.
(86) Meyer, K.; Mindiola, D. J.; Baker, T. A.; Davis, W. M.; Cummins, C. C. *Angew. Chem., Int. Ed.* **2000**, *39*, 3063–3066.
(87) Connelly, N. G.; Kitchen, M. D. *J. Chem. Soc., Dalton Trans.* **1977**, 931–937.
(88) Zwickel, A.; Taube, H. *J. Am. Chem. Soc.* **1961**, *83*, 793–796.
(89) Brown, G. M.; Sutin, N. *J. Am. Chem. Soc.* **1979**, *101*, 883–892.
(90) Halpern, J. *Q. Rev.* **1961**, *15*, 207–236.
(91) Stranks, D. R. *Discuss. Faraday Soc.* **1960**, *29*, 73–79.
(92) Wahl, A. C.; Deck, C. F. *J. Am. Chem. Soc.* **1954**, *76*, 4054–4055.
(93) Andersen, R. A.; Chisholm, M. H.; Gibson, J. F.; Reichert, W. W.; Rothwell, I. P.; Wilkinson, G. *Inorg. Chem.* **1981**, *20*, 3934–3936.
(94) Hayton, T. W.; Boncella, J. M.; Scott, B. L.; Batista, E. R.; Hay, P. J. *J. Am. Chem. Soc.* **2006**, *128*, 10549–10559.
(95) King, R. B. *Inorg. Chem.* **1992**, *31*, 1978–1980.
(96) King, R. B. *Inorg. Chem.* **1998**, *37*, 3057–3059.
(97) Bain, G. A.; Berry, J. F. *J. Chem. Educ.* **2008**, *85*, 532.
(98) *SMART Software User's Guide*, Version 5.1; Bruker Analytical X-Ray Systems, Inc.: Madison, WI, 1999.
(99) *SAINT Software User's Guide*, Version 5.1; Bruker Analytical X-Ray Systems, Inc.: Madison, WI, 1999.
(100) Sheldrick, G. M. *SHELXTL*, 6.12; Bruker Analytical X-Ray Systems, Inc.: Madison, WI, 2001.
(101) Frisch, M. J.; et al. . *Gaussian 09*, Revision A.02; Gaussian, Inc.: Wallington CT, 2009.
(102) Becke, A. D. *J. Chem. Phys.* **1993**, *98*, 5648–5652.
(103) Stephens, P. J.; Devlin, F. J.; Chabalowski, C. F.; Frisch, M. J. *J. Phys. Chem.* **1994**, *98*, 11623–11627.
(104) Petersson, G. A.; Bennett, A.; Tensfeldt, T. G.; Al-Laham, M. A.; Shirley, W. A.; Mantzaris, J. *J. Chem. Phys.* **1988**, *89*, 2193–2218.